Memory System Maladaptation Impairs CA1-Dependent Temporal Binding and Declarative Memory in the Cntnap2 Knockout Mouse Model of Autism

Elise C. Rawlinson[1], Michael H. McCullough[1,2], Azza Sellami[3,4], Aline Marighetto[3,4], A. Shaam Al Abed[1,5*#], Nathalie Dehorter[1,5*#]

Abstract

Growing evidence implicates the hippocampus in the pathophysiology of autism spectrum disorder, particularly in the domains of social interactions and cognition. Yet, the mechanisms driving hippocampal-dependent cognitive atypicalities in autism remain poorly defined. Here, we characterize how dysfunction of the CA1 subfield of the dorsal hippocampus (dCA1) impacts critical components of declarative memory. Using trace fear conditioning combined with *in vivo* fiber photometry in the *Cntnap2* knockout mouse model of autism, we found that capabilities to bridge temporally distant stimuli, i.e. temporal binding capabilities, were reduced relative to wildtype mice. This impairment was associated with decreased dCA1 activity during temporal gaps. Using a relational/declarative memory task, we also revealed a deficit in flexible spatial memory, a preferential use of egocentric learning strategy. This unflexible learning strategy resulted from the imbalance between memory system activity, promoting frontostriatal-dependent procedural learning instead of dorsal dCA1/hippocampus-dependent relational/declarative memory. Overall, this study elucidates how memory systems are mistuned in the *Cntnap2* knockout mouse model, opening new avenues for understanding and addressing atypical learning in autism.

Affiliations:

[1] Eccles Institute of Neuroscience, John Curtin School of Medical Research, The Australian National University, Canberra, ACT, Australia

[2] School of Computing, The Australian National University, Canberra, ACT, Australia

[3] Neurocentre Magendie, Physiopathologie de la plasticité neuronale, U1215, INSERM, F-33000 Bordeaux, France

[4] Université de Bordeaux, F-33000 Bordeaux, France.

[5] The Queensland Brain Institute, The University of Queensland, Brisbane, QLD, Australia

[*] These authors contributed equally to the work and are listed alphabetically

[#] Co-corresponding authors: A. S. Al Abed (shaam.alabed@anu.edu.au) and N. Dehorter (n.dehorter@uq.edu.au), The Australian National University and The University of Queensland.

Key words: Autism, episodic memory, hippocampus, dCA1

Abbreviations: ASD: Autism Spectrum Disorder; KO: Knock-Out; WT: Wildtype

Introduction

Autism spectrum disorder (ASD) is a lifelong neurodevelopmental disorder comprising difficulties in social behavior, atypical communication skills, and the presence of restricted or repetitive behaviors or interests [1]. Beyond these core features, individuals with ASD present with difficulties in cognitive domains which can impact daily functioning and adaptability. In particular, people with ASD present with atypicalities in episodic/declarative memory [2], the ability to recall specific events and experiences (i.e., *what happened when and where*). Yet, the underlying neurological mechanisms of declarative memory impairments in ASD remain to be fully elucidated.

While most research has focused on the dysregulation of the prefrontal cortex and the basal ganglia in ASD, recent studies have highlighted that hippocampal defects are key in the social domain of this phenotype. [3–6]. In addition, the hippocampus is known to play a critical role in declarative memory by forming temporally and spatially organized relational representations of past experiences, allowing flexible expression of memories [7]. The dorsal CA1 subfield (dCA1) plays a key role in this relational process, by sustaining the ability to link temporally distant events, called temporal binding [4, 8]. A relational binding account of episodic memory difficulties has been proposed for autistic individuals, positing a selective weakness in hippocampus-dependent binding of items and contexts, while memory for items alone remains relatively spared [9, 10]. In parallel to this relational hypothesis of memory atypicalities, time estimation tasks in individuals with ASD have shown that disruptions in integrating temporal information affect the development of temporal relationships [11–13]. In this context, we hypothesized that dCA1 activity related to temporal binding could be impaired in ASD, leading to declarative memory defects.

Here we examine this hypothesis in the *Cntnap2* knock out (KO) mouse model of ASD, that exhibits autism-like phenotypes, including social behavior deficits [14, 15]. Animals were assessed in two behavioral paradigms: first, trace fear conditioning, a simple temporal binding-dependent memory task allowing the simultaneous recording of dCA1 activity; second, a radial maze task which models the complexity of temporal binding-dependent relational/declarative memory. We demonstrate that *Cntnap2* KO mice present with mistuned dCA1 activation and abnormal reorganization of memory systems during temporal binding-dependent memory formation.

Results

Cntnap2 KO mice demonstrate reduced temporal binding capability.

We tested temporal binding capabilities of *Cntnap2* KO mouse model using the trace fear conditioning paradigm (TFC; **Fig. 1A**), in which mice are required to memorize the association between a tone (Conditioned Stimulus) and a mild electric foot-shock (Unconditioned Stimulus), separated by a time interval called *Trace* [8]. In the first stage, i.e., the conditioning, independent groups of mice were exposed to three tone-shock pairings with a trace interval between 5 and 60 sec (*i.e.* T5, T20, T40, and T60; **Fig. 1A**). All groups showed intact conditioning abilities, demonstrated by increasing freezing times [16] during the tone and traces periods (**Fig. 1B**). 24h later, the animals were re-exposed first to the conditioned *tone* in a neutral context (*i.e.* tone test) to assess efficiency of temporal binding reflected in fear response (% time freezing) to the tone, and second to the conditioning *context* alone, to evaluate contextual memory. As previously demonstrated [8, 17], WT mice displayed efficient temporal binding capacity up to a 40 sec trace interval (**Fig. 1C**), illustrated by strong and specific fear response to the tone in a neutral context (**Fig. 1C**). Interestingly, *Cntnap2* KO mice also displayed a strong and specific freezing to the tone for up to a 20 sec trace interval (**Fig. 1C**, T20), but not for 40 sec (**Fig. 1C**, T40), indicating reduced temporal binding capacity compared to WT mice. A precise memory includes the ability to distinguish between two contexts: conditioning context and neutral context. While all (but T60) WT groups showed such context discrimination, *Cntnap2* KO mice presented with lower (or no) context discrimination (**Fig. 1D**). Taken together, our results demonstrate that *Cntnap2* KO mice display poor contextual discrimination and reduced temporal binding capacity.

Mistuning of dorsal CA1 activity during temporal binding in *Cntnap2* KO mice.

Whilst alterations in item binding in ASD have already been reported, the underlying mechanisms have not been described [9]. Knowing that sustained activity of dCA1 neurons during time intervals is needed for temporal binding [8, 17], we here dissected dCA1 activity during temporal binding in *Cntnap2* KO mice. We recorded calcium transients during encoding and recall of trace fear conditioning, using fiber photometry in animals trained under the 40s-trace interval (**Fig. 2A, B**). As in Fig. 1, both WT and *Cntnap2* KO mice implanted with an optic fiber could associate the tone and the shock, reaching a high level of freezing after 3 tone-shock pairings (**Fig. 2C**). While the frequency of the calcium transients did not differ between WT and C*ntnap2* KO mice throughout conditioning (**Fig. 2D-E**), their amplitude was significantly reduced both during the presentation of the second tone and consistently across the 3 trace intervals in *Cntnap2* KO mice (**Fig. 2E, G**). These results suggest a lack of

synchronized neuronal activity, as previously reported [18]. They also suggest that sustained activity of dCA1 neurons during the trace interval, which is seen in WT but not *Cntnap2* KO mice, supports temporal binding enabling adequate memorization of the association between the 40s-distant tone and shock despite their temporal separation.

In the tone test, as in Fig. 1C, *Cntnap2* KO mice failed to express a fear response to the tone attesting of impaired trace fear memory and temporal binding ability, relative to WT mice (**Fig. 2F**). While the frequency of calcium transient remained unchanged (**Fig. 2I**), the amplitude of the peaks was lower during the tone presentation and the subsequent trace period in *Cntnap2* KO compared to WT mice (**Fig. 2J**). Further analysis of calcium activity during the tone test showed a large calcium transient approximately 6 seconds after the tone onset in WT mice (**Fig. 2K**), which was preceded by a peak of freezing. The dCA1 activity post-freezing could therefore reflect the integration of freezing sensory feedback. In contrast, a similar peak of freezing in *Cntnap2* KO mice (starting approximately 3 sec post tone presentation) did not result in increased dCA1 activity, potentially indicating an absence of sensory integration. During the trace period of the tone test, *Cntnap2* KO mice displayed significantly lower average activity (**Fig. 2L**), compared to WT mice. This result further supports that the reduction of temporal binding capacity in *Cntnap2* KO mice stems from a lack of sustained dCA1 activity during encoding and recall of the tone-shock association.

Egocentric learning and inflexible long-term memory in *Cntnap2* KO mice

Following the observation that *Cntnap2* KO mice present with reduced dCA1 activity related to temporal binding capabilities, we dissected declarative memory atypicalities. We employed a radial maze task modeling the complexity of temporal binding-dependent relational/declarative memory [19]. This task assesses the characteristic flexibility of R/DM expression which relies on dCA1-dependent capability to relate temporally distant events [8]. To do so the R/DM task is divided into two stages: acquisition and flexibility test (**Fig. 3A**). In the acquisition stage, mice are trained daily to learn the food-reward location within 3 separate pairs of adjacent arms. After reaching the learning criterion (>75% correct choices of rewarded arm), the flexibility of the memory learnt during acquisition is probed by recombining 2 pairs, without changing the position of the reward (pairs A and B recombined into Pair AB; **Fig. 3A**). Cumulative evidence has shown that flexibility lies upon hippocampus-dependent relational representation of separate experiences made on each pair during the acquisition phase [8, 17, 20]. To impose a temporal binding demand on relational memory acquisition, each pair presentation is separated by a 20s inter-trial interval [8].

Both wild-type (WT) and *Cntnap2* KO mice were able to acquire the task (**Fig. 3B**). *Cntnap2*

KO mice tended to take more days (**Fig. 3C**) and reached higher levels of performance on the last of training (**Fig. 3B**, right panel). In the flexibility test, their performance dropped significantly between the last training session and the flexibility test (stage 2 of the R/DM task), and *Cntnap2* KO mice performed significantly lower than WT in the critical test of flexibility (**Fig. 3C-Recombined pair AB**). In contrast, both groups performed similarly on the control pairs: unchanged pair C, with high performance **(Fig. 3D)**, and the new pair N, at chance levels **(Fig. 3E).** How can we explain the lack of flexibility? We have previously shown that the flexibility component of R/DM depends on the learning strategy used during the acquisition stage: allocentric spatial mapping/relational or egocentric/procedural, the latter leading to lateralization. Indeed, if the use of spatial cues is impaired in any case of hippocampus damage/dysfunction, mice will use a left-right egocentric strategy to memorize reward locations, leading to unflexible memory [8, 20]. Therefore, the chance-level flexibility performance of *Cntnap2* KO mice suggests a bias towards a procedural learning strategy, in line with the well-documented prominence of behavioral inflexibility in ASD [21]. This was confirmed by analyzing lateralization during acquisition by comparing performance on left-baited pairs (Pairs A and B), *vs.* right-baited pair C (Method, **Fig. 3F**). *Cntnap2* KO mice displayed significantly more lateralization than WT, meaning that they used an egocentric procedural strategy to learn the position of the food reward rather than using spatial mapping like WT mice. Interestingly, *Cntnap2* KO mice had quicker decision times than WT **(Fig. 3G)**. This is in line with the well-demonstrated impulsiveness in ASD (DSM-5). In addition, WT mice demonstrated a longer time to enter a non-baited arm compared to a baited arm, suggesting that they somehow know before entering the arm whether it is the rewarded one or not, and therefore, base their decision on deliberation and precise spatial representation. In contrast, *Cntnap2* KO mice had similarly short latencies whatever their responses suggestive of non-reflexive decision, impulsive automatic responses and impaired spatial representation of reward information. In addition, once their choice decision was taken, their runtime (from the central platform to the end of the arm) was longer than that of WT's (**Fig. 3H**), implying that only deliberative processes were shortened/absent in KO mice and slowing down run possibly is a compensation for impulsive decisions. Altogether, we show that *Cntnap2* KO mice present with a lack of flexible memory expression modeling a relational/declarative memory impairment and associated with preferential use of an egocentric/procedural learning strategy.

Shift towards striatum-centered activities in *Cntnap2* KO mice

Each learning strategy is known to depend on partially distinct brain systems: hippocampus-dependent supporting allocentric spatial/relational learning, or striatum-based leading to egocentric/procedural learning [22]. To assess the learning-induced activity of these different

structures, we quantified the levels of the cellular activity marker cFos after day 3 of R/DM task acquisition in structures involved in memory (dorsal hippocampus (dCA1, dCA2, dCA3, dorsal dentate gyrus (dDG); dorso-medial (DMS) and dorso-lateral striatum (DLS); Prefrontal cortex (infralimbic (IL), prelimbic (PrL), and anterior cingular (ACC); **Fig. 4A**). As previously shown [8, 17], we found a significant activation of dCA1 in trained WT mice compared to naïve WTs, consistent with the use of an allocentric/spatial learning strategy [22] **(Fig. 4B)**. In contrast, there was a lack of learning-induced dCA1 activation in the *Cntnap2* KO mice, combined with an hypoactivation of dCA3 in both naïve and trained groups compared to WT. This lack of hippocampal activation likely underlies the deficit in temporal binding and spatial learning capabilities in this task **(Fig. 3C)**. Moreover, *Cntnap2* KO mice displayed a significant activation in the DMS with training compared to their naïve controls that was not replicated in the WT mice **(Fig. 4C)**. No other significant changes were seen in any of the other prefrontal cortex structures measured (DLS, IL, PrL, ACC; **Fig. 4D)**. Together, this supports the central involvement of the DMS in egocentric learning strategy of *Cntnap2* KO mice.

To further dissect the balance between memory systems, we analyzed the weight of each structure within the total activation of the system (**Fig. 4E-F**). After training, we found a disproportionate representation of the PFC and striatum over the hippocampus in *Cntnap2* KO mice compared to WT (**Fig. 4E**). Indeed, in comparison to WT naïve mice, WT trained mice exhibited an increase in the weight of the dCA1 in the network activity n, likely supporting temporal binding and through ensuing relational organization of the 20s-distant pair presentations, the formation of flexible memory. In contrast, no such reorganization of activities in the network was observed in *Cntnap2* KO mice with training (**Fig. 4F**). Differences in the weight of each sub-structures in trained WT vs *Cntnap2* KO mice affected the dCA1, dCA2, and dCA3, in favor of DMS, IL, and ACC. Overall, we found a compensatory activation of the frontal-striatal structures concomitant with hippocampal hypoactivation.

In addition to the learning-induced activity of individual structures, the pairwise correlation of activity between structures enhances our understanding of network-wide synchronization. While WT naïve mice presented with mainly positive correlations between the striatum, PFC, and hippocampus, aside from the dDG being negatively correlated with the PFC, naïve *Cntnap2* KO mice displayed mainly negative correlations (**Fig. 4G**). This indicates that, by default, the between-structure relationships are dysregulated in *Cntnap2* KO mice, preventing the use of a hippocampus-based learning strategy. Altogether, the analysis of learning-induced brain activity demonstrates a shift towards striatum-centered activity and connectivity in *Cntnap2* KO mice, likely leading to egocentric learning strategy and inflexible memory.

Discussion

This study delved into changes in memory processing in the *Cntnap2* KO mouse model of ASD, revealing that compromised dCA1 hippocampal activity disrupts temporal binding capabilities and through ensuing defects in relational processing of temporally distant events, leads to deficits in declarative memory. Additionally, we found that hippocampal dysfunction in *Cntnap2* KO mice shifts the brain's focus toward striatum-dependent egocentric learning.

Interplay between hippocampus and striatum in memory deficits in *Cntnap2* KO mice.

Atypicalities in declarative memory have been reported in ASD, with specific impairments in relating items [9]. Here we demonstrate a reduction in dCA1-dependent temporal binding capacity in *Cntnap2* KO mice, which can contribute to the declarative memory impairment by disrupting the relational organization of temporally distant events. Indeed, in the trace fear conditioning experiments, *Cntnap2* KO mice showed efficient temporal binding with time intervals up to 20s instead of 40s in WT mice and this reduction was associated with a reduction of dCA1 activity during the encoding and recall of the 40s-trace fear conditioning. Temporal integration of stimuli relies on hippocampal activity, in particular that of dCA1 [8, 23–25]. Similarly, we found an impaired activation of the dCA1 in *Cntnap2* KO mice during the acquisition of the R/DM task (**Fig. 4B**). The lack of training-induced dCA1 activation likely prevents the generation of fine-tuned temporal integration of distant events leading to flexibility deficits [8, 20, 26, 27]. Moreover, analysis of broader memory systems' activity during encoding revealed an aberrant recruitment of the DMS in the *Cntnap2* KO mice, paired with an altered pair-wise correlation between activation of related brain regions (**Fig. 4G**). Indeed, as opposed to the positive correlations observed in WT mice, we found a negative correlation between the DLS, the prefrontal cortex and hippocampus in *Cntnap2* KO mice. This profile was found in naïve groups, suggesting that the bias towards lateralized learning strategy stems from baseline mistuning of the functional connectivity between brain structures necessary for spatial learning in ASD. This shift towards a striatum-centered system also implies a predominance of an unconscious encoding, in which relations between items are learnt via stimulus-response, leading to inflexible goal-directed actions, resemblant of habits [28].

Decoding spatial and temporal maps in autism.

The dCA1 region is recruited with other hippocampal areas to form and maintain spatial, temporal and social maps, which are mental relational representations of our environment [6]. dCA1 neurons contribute to encoding and recalling spatial information, enabling individuals to navigate and understand their surroundings. Specific "time cells" create a temporal framework that supports episodic memory, encoding of the passage of time and the prediction of future

events [4]. Recent research also suggests that CA1 plays a role in social cognition via so-called "social maps" to process and recall social information that is essential for effective social behavior and social dynamics [29]. There is limited information on how cognitive deficits evolve over time and their long-term effects in ASD. It would be of interest to further address how specific maps are formed and maintained in this condition.

The role of dCA1 in spatial representations has been profusely documented. Consistently, we recently demonstrated the central role of dCA1 in the maladaptive contextual encoding in post-traumatic stress disorder (PTSD), i.e., the degradation of declarative memory surrounding a highly stressful event [1, 30, 31]. Interestingly, growing evidence reports the propensity to develop PTSD in ASD [32, 33], suggesting that the lack of dCA1 activation impacts cognition beyond everyday learning. Together, these studies further elaborate on the crucial role of the hippocampus as a promising target to alleviate ASD pathophysiology.

To obtain a deeper understanding of the hippocampus' computation underlying memory formation, we analyzed the correlation between neuronal dynamics and behavioral outcomes within the fear memory test. Fiber photometry recordings in the dCA1 showed that whilst WT mice displayed sustained hippocampal activity during memory trace (**Fig. 2J, L**), hippocampus-dependent memory systems were not similarly activated in the *Cntnap2* KO mice (**Fig. 4B; Fig. 2J, L**). We found largely decreased amplitude of the calcium transients (**Fig. 2**), paired with a loss of key peaks of activation (*e.g.* 6 sec post sound), which no longer correlated with freezing behavior. This overall suggest that the deficits in temporal binding and declarative memory originate from a decrease in hippocampal neuronal synchronization and dynamics Nevertheless, we found that hippocampus-dependent memory systems were not activable in the *Cntnap2* KO mice, contrary to WT mice which displayed sustained hippocampal activity during memory trace (**Fig. 2L**). In the same line, a recent study reported during contextual fear conditioning, that neurons allocated to the memory trace displayed specific activity compared to non-allocated neurons [34]. While our study design does not provide these details, the lack of active cells in the dCA1 during acquisition of the relational/declarative memory task could imply an allocation of the memory trace of the reward location within the striatum, instead of the hippocampus [35]. Further experiments are needed to determine whether atypical engram allocation is linked to learning strategies in ASD.

Aged-like performance suggests early cognitive decline in autism

In this study, we demonstrate the disruption in hippocampal and dCA1 functioning in the *Cntnap2* KO mice, a hallmark of memory defects observed during aging [36, 37]. Consistent with reports suggesting that people with autism are at risk of premature cognitive aging [38],

we have found that young adult *Cntnap2* KO mice exhibit a memory profile similar to those of aged WT mice [8, 17, 39]. Compared to young WT mice, both groups showed flexibility impairments in the relational/declarative radial maze task, and both exhibited a striatum biased learning strategy. Yet, the underlying mechanisms driving these deficits remain unknown. We previously demonstrated that dCA1 activity during the temporal gaps was necessary to link separate pairs into a relational/flexible memory [8, 17] and specific dCA1 optogenetic activation during time intervals increases temporal binding capacity, rescuing R/DM formation. Given that CA1 neurons are less synchronized in ASD, targeted dCA1 activation could alleviate memory deficits. We propose that fine-tuning dCA1 activity may normalize memory system balance, offering a novel therapeutic approach for cognitive impairments in ASD. Further delineation of associated connectomes [40] could provide insights into targeted brain circuit therapies. Autism is a highly heterogeneous condition, with individuals presenting a wide range of atypical cognitive abilities. As such, the extent and nature of memory deficits can vary greatly among individuals. Research has yet to fully elucidate how memory deficits manifest across the spectrum of autism, including the interplay between memory impairments and other cognitive features such as attention, executive functioning, and language. A better understanding of these individual differences is necessary to create more personalized and effective interventions. Further studies in different animal models will be necessary to fully comprehend the common cognitive mechanisms at play in autism.

Methods

Mice

3 to 5-month-old naive mice were collectively housed in standard Makrolon cages, in a temperature- and humidity-controlled room under a 12h light/dark cycle (lights on at 07:00), with *ad libitum* access to food and water. We used both males and females to minimize the number of mice produced in this study. WT and *Cntnap2*$^{-/-}$ KO mice (Jackson ID: #017482 [15]) were non-littermates, derived from breeders of the same colony and used for behavior and histological analyses. All experiments took place during the light phase. We replicated the behavioral experiments in two to four different batches. Every effort was made to minimize the number of animals used and their suffering. All procedures were conducted in accordance with the European Directive for the care and use of laboratory animals (2010-63-EU) and the animals care guidelines issued by the animal experimental committee of Bordeaux University (CCEA50, agreement number A33-063-099; authorization N°21248), and from the Australian National University Animal Experimentation Ethics Committee (protocol numbers A2018/66, A2020/26, and A2021/43).

Trace fear conditioning task (TFC)

Apparatus: Fear conditioning behavior was performed in a Plexiglas conditioning chamber (20 x 20 x 30 cm), in a brightness of 100 lux, given access to the different visual-spatial cues in the experimental room. The floor of the chamber consisted of stainless-steel rods connected to a shock generator (Imetronic, Pessac, France).

Trace fear conditioning procedure: The box was cleaned with 70% ethanol before each trial.

During acquisition of conditioning, each animal received 3 pairings of a tone (70 dB, 1 kHz, 30 s) and a footshock (0.3 mA, 50 Hz, 1 s). The two stimuli were separated by a trace interval of 5, 20, 40 or 60 sec, depending of the group.

All mice were submitted 24 hour later to the *Tone retention test* during which they were re-exposed to the tone alone in a dark and modified chamber [2min pre-tone, 2min tone and 2min post-tone]. A context test was also performed 2 hours later, during which mice were re-exposed to the conditioning chamber alone during 6 min.

Animals were continuously recorded for off-line scoring of freezing, by an experimenter ignorant of the experimental condition/group. Freezing is defined as a lack of all movement except for respiratory-related movements. Acquisition of the TFC was measured by the progression of freezing during the tone across the 3 tone deliveries. 24h-retention of the trace association was measured during the tone test by the evolution of percentage of freezing time.

Radial-maze task of (Relational/) Declarative memory (DM)

Apparatus: We used an open 8-arm radial maze made of grey Plexiglas, automatized by videotracking (IMETRONIC – Pessac, France). The diameter of the central platform is 30 cm and the arms are 55 cm long by 10 cm large. Each arm is equipped with a door at its entrance and a food-pellet delivering system at its end. The doors are individually controlled (raised up or dropped down) by the computerized system which also controls pellets availability in the food tray at the end of each arm individually, according to the task. The maze is placed in an empty room containing visual cues to enable spatial discrimination.

Behavioral Procedure: During the entire procedure, animals were submitted to one daily session. Prior to memory testing, animals were habituated to the apparatus over a period of two days during which animals were allowed to move freely in the radial maze. To complete the session, mice had to visit each arm until its end. Choice accuracy was measured as the percentage of correct responses for each pair.

Stage 1: Acquisition of 3-pair discriminations

The acquisition task consisted in learning the position of the food within the maze. Indeed, each animal was assigned three adjacent pairs of arms (pairs A, B and C). In each pair, only one arm was baited as a food reward. The experiment is designed in a way that the left arms of

the pairs A and B are baited while the right arm of the pair C is. In each trial, mice were given access to a pair (either pairs A, B and C). A choice was considered to be made when the subject had reached the food well of an arm; this also closed the door of the non-chosen arm. The trial was finished as soon as the animal returned to the central platform. The subject was then confined to the central platform for 20s before the next discrimination trial began: this constituted the inter-pair interval. Each daily session consisted of 20 consecutive trials comprising alternate presentations of pairs A, B and C according to a pseudo-random sequence.

A mouse was considered to reach criterion when its overall choice accuracy was at or above 75% over two consecutive sessions given that performance in each of the three discrimination choices were at least 62% correct. The test task began the following day when criterion performance was reached.

Lateralization index was quantified by using the absolute value of the subtraction of the performance on the left-baited pairs vs. the right-baited pairs. Lat = |((Pair A + Pair B) /2) - Pair C|. We then used the maximum lateralization over 3 consecutive days.

Stage 2: Flexibility probe of DM

In the test task, the position of the food in the maze did not change, but characteristic flexibility of DM expression was assessed by changing the way of presenting the arms. Indeed, in place of the pairs A and B, a pair AB was submitted to the mouse. The AB pair consisted in the combination of the two adjacent arms of the pairs A and B. It was the critical test of flexibility. Two other pairs were used as control: the pair C that remained unchanged ("unchanged learnt control", and pair N (=new) made of the two arms non-used in acquisition ("unlearnt control").

FiberPhotometry. *Surgery:* Mice were injected unilaterally 4 weeks before behavioral experiments with an Adeno-Associated Virus (AAV) GCaMP6f (AAV1-hsyn- jGCaMP6f-WPRE, Addgene). We used glass pipettes (tip diameter 25-35 µm) connected to a picospritzer (Parker Hannifin Corporation) into the right side of the dorsal CA1 of the hippocampus (0.1 µl/site; AP -1.8 mm; L +1.35 mm; DV -1.4 mm). Mice were then implanted with unilateral optic fiber implant (diameter: 200µm; numerical aperture: 0.39; flat tip; Neurophotometrics). Implants were fixed to the skull with Super-Bond dental cement (Sun Medical, Shiga, Japan). Mice were perfused after experiments to confirm correct placements of fibers (**Fig. S4c-e, g**). Viral injections targeted the pyramidal cell layer of the dCA1.

Recordings: Data were recorded using a Neurophotometrics FP3002 system (Neurophotometrics, San Diego, CA). Briefly, 470 and 415 nm LED light was bandpass filtered, reflected by a dichroic mirror, and focused onto a multi-branch patch cord (Neurophotometrics, San Diego, CA) by a x20 objective lens. Alternating pulses of 470 and 415 nm light (~50 µW) were delivered at 60 Hz, and photometry signals were time-locked to

behavior using a Bonsai workflow. Signals were analyzed using the Synaptech suite cloud service (MetaCell) and custom-made Python scripts (Code available at https://github.com/elisecr/fiberphotometry_2024). Through the Synaptech platform, 470 and 415 signals were deinterleaved. For all experiments except context and tone test, the exponential delay period (the first 10 seconds REF) of the recording were removed. To correct for photobleaching, isosbestic (415nm) signals were fit to a biexponential curve to model the baseline signal with photobleaching. The fitted biexponential curve was then scaled to match the 470nm signal using non-negative robust linear regress, and subtracted from the 470 trace to correct for baseline drift. Traces were then Z scored.

Experimental traces: Z scored data were analyzed by custom python scripts to extract calcium fluorescence traces for each experiment. For the trace fear conditioning experiments, these data were aligned to files generated by the poly fear software (Imetronic, France) ".dat" files to align the beginning of the tone and shock events to the closest millisecond in the Z scored data. These were then extracted to provide traces for each event of interest. For the context and tone test, the first 10 seconds of the experiment was also represented in the trace. For the tone test, the timing of the tone was extracted as described above to accurately align the data.

Peak finding: The threshold for peak analysis definition was set at 1.0. Peak analysis was conducted using a custom-built Python script to calculate peak frequency and amplitude.

Behaviour analysis: Timestamps of behavior of interest for each experiment, including freezing, were manually coded during the experiment. Through the synaptech platform, these were then aligned to this Z scored data to provide bouts of behavior. These bouts were defined by a minimum separation of 0.5s and minimum duration of 0.3s. Bouts of digging and grooming were then extracted by custom built python scripts to quantify the duration of each behavior over relevant experiments. Bouts of interaction with object and mouse in social preference experiments were also quantified as previously described. In the Synaptech pipeline, defined bouts were then analyzed for the area under the curve (AUC) and mean for 10 seconds before, during and 40 seconds after bouts. Custom Python scripts were created to average and display these data. Code available at https://github.com/elisecr/fiberphotometry-analysis

Immunohistochemistry. Animals were perfused transcardially 90 min after the flexibility test on Day 3 for c-Fos analysis with 0.01M phosphate buffered saline (PBS) to eliminate blood and extraneous material, followed by 4% paraformaldehyde (PFA). Brains were postfixed for 36h in PFA. Tissues were sectioned at 40 µm using a Leica 1000S vibratome and kept in a cryoprotective ethylene glycol solution at -20˚C until processed for immunofluorescence. Sections were first washed and permeabilized in PBS-Triton 0.25%, then non-specific binding

sites were blocked by immersing the tissue in 10% normal donkey serum, 2% bovine serum albumin in PBS-Triton 0.25% during 2h. Tissues were then stained using the primary antibodies overnight: mouse anti-c-Fos (1:1000; Santa Cruz). After 3x 15 min washes, we added anti-rabbit Alexa 488 (1:200; Life Technologies) secondary antibodies for 2h. After 3x 15 min washes slices were stained during 5 min with DAPI (5µM; Sigma), mounted on Livingstone slides then covered with Mowiol (Sigma) and coverslip (Thermofisher). c-Fos, staining from 2-3 slices par animals were imaged using a Nikon Axioscan confocal fluorescent microscope (20x objective). Stained sections of WT and mutant mice were imaged during the same imaging session. Immunofluorescence signals were quantified using the quPath software with routine particle analysis procedures (size= 30-500; circularity=0.30-1.00), to obtain nuclear masks, divided by the area to obtain cell density per mm^2.

Statistics. Data are presented as mean ± SEM. Statistical analyses were performed using GraphPad prism or StatView software for 2-way ANOVA, followed by Bonferroni *post-hoc* test or Student's t test, when appropriate. Normality of the data was confirmed using the Kolmogorov–Smirnov test. Statistical significance was considered at $p<0.05$.

Data availability

All data is available in the main text. Raw data will be made available upon reasonable request. Code available at https://github.com/elisecr/fiberphotometry_2024

Acknowledgments

We thank all the personnel of The Australian Phenomics Facility and of The Neurocentre Magendie involved in mouse care.

Funding

Australian National University Futures scheme, NHMRC Ideas Grant 2019416, Centre National pour la recherche scientifique (CNRS), Bordeaux University, L'institut national de la santé et de la recherche médicale (INSERM), the John Curtin School of Medical Research.

Author contributions

Conceptualization: ASA;
Methodology: ASA, ND, AM, MHM;
Investigation: ASA, ECR
Writing—original draft: ASA, ND
Writing—review & editing: ND, ASA, AM, ECR, MHM

Competing interests

Authors declare that they have no competing interests.

Figures and Legends

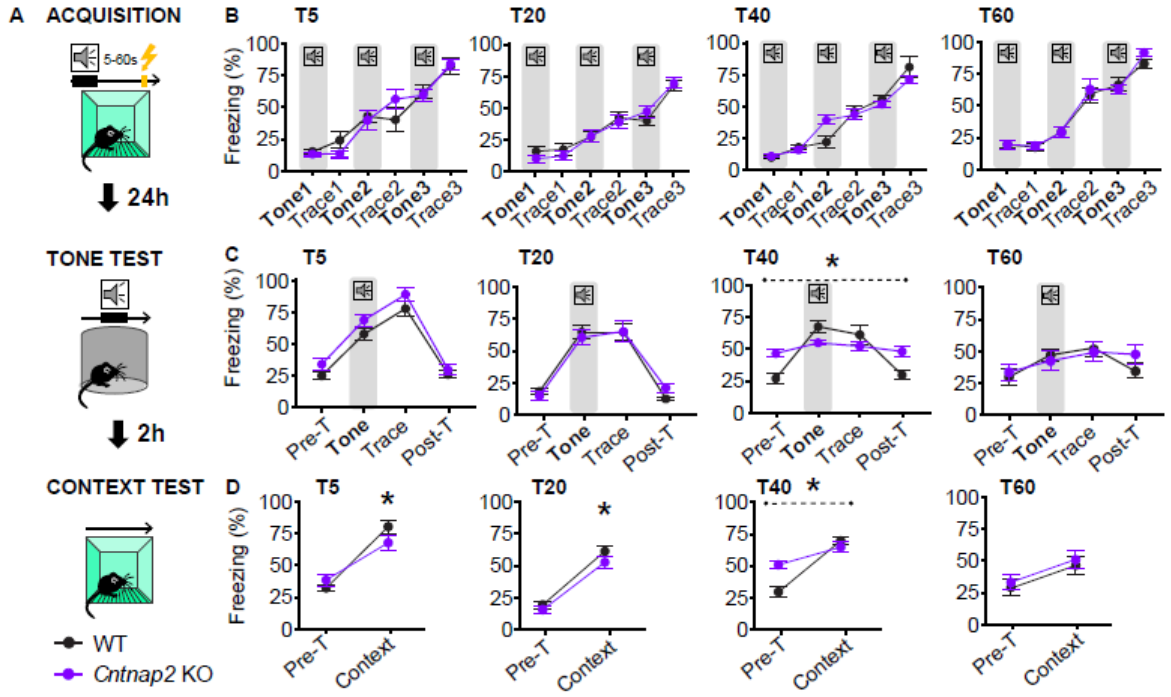

Figure 1. *Cntnap2* KO display reduced temporal binding capabilities

A. Experimental design: Trace Fear Conditioning includes a conditioning session in which mice have to associate a tone and a shock, separate by a time interval (trace). Independent groups of mice were trained with trace intervals of 5, 20, 40, or 60 seconds (T5: WT n=10; KO n=11; T20: WT n=12; KO n=12; T40: WT n=12; KO n=14; T60: WT n=10; KO n=9). **B.** Freezing levels (percent) during the conditioning session for WT (black) and *Cntnap2* KO (purple) groups, conditioned with distinct trace durations. **C.** Freezing levels (percent time freezing) during the pre- tone, tone, trace and post-trace periods in the tone test for WT (black) and *Cntnap2* KO (purple) groups, 24h post-conditioning with distinct trace durations (T40: Pre-tone: p=0.0005; Genotype x Freezing interaction: $F_{3, 72}$=12.671; p<0.0001). **D.** Freezing levels (percent time freezing by 2 min) in the neutral context (pre-tone period, pre-T in the tone test) and in the conditioning context (context test) for WT (black) and *Cntnap2* KO (purple) groups, 24h post-conditioning with distinct trace durations (T20: p=0.0281in context test; T40 ???).

Data shown at mean ± SEM. *: p<0.05.

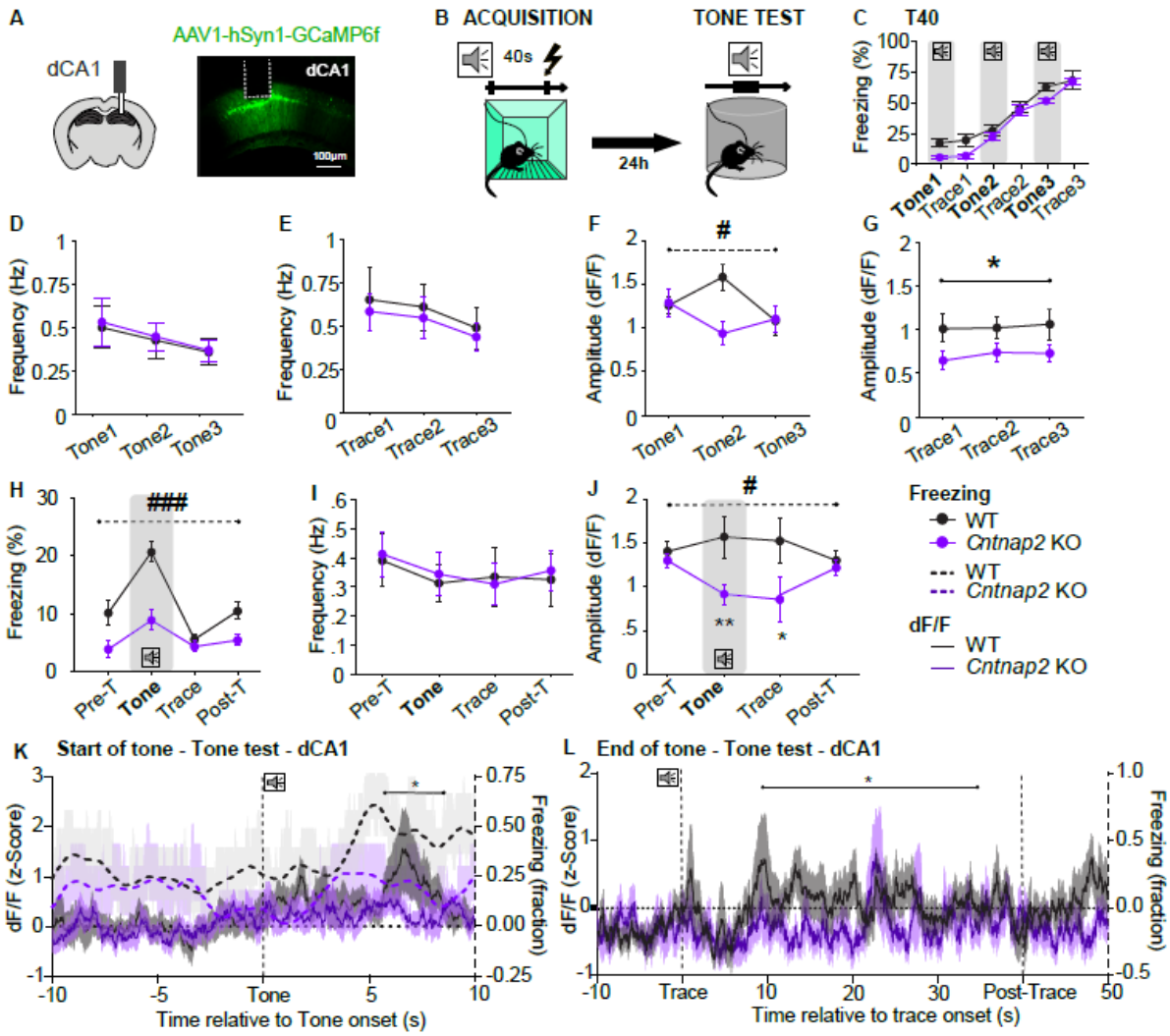

Figure 2. Altered calcium responses during fear conditioning and recall in *Cntnap2* KO

A. Left panel: scheme depicting the fiber optic implantation targeting the dorsal CA1 subfield of the hippocampus (dCA1). Right panel: Representative image of the optic fiber placement, in the pyramidal cell layer of the dCA1, scale: 100µm. Calcium activity was recorded using the calcium indicator GCaMP6f. **B.** Experimental design: Mice were trained in the Trace Fear Conditioning paradigm under a 40s trace interval, followed by a tone test 24h later. **C.** Freezing levels (percent) during acquisition for WT (black) and *Cntnap2* KO (purple) groups, conditioned with a 40s trace interval (T40). **D.** peak frequency of Ca^{2+} transients during the 3 tone presentations of the conditioning (ns). **E.** peak frequency of Ca^{2+} transients during the 3 trace intervals of the conditioning (ns). **F.** peak amplitude of Ca^{2+} transients during the 3 tone presentations of the conditioning (Genotype x Tone interaction: p=0.0247; WT n=11; KO

n=10). **G.** peak amplitude of Ca^{2+} transients during the 3 trace intervals of the conditioning (Genotype: p=0.0408; WT n=11; KO n=10). **H.** Freezing levels (percent) during the tone test for WT (black) and *Cntnap2* KO (purple) groups, 24h post-conditioning (Genotype x Tone interaction: p=0.0007; WT n=11; KO n=10). **I.** Peak frequency of Ca^{2+} transients across the tone test (ns). **J.** Peak amplitude of Ca^{2+} transients across the tone test (Genotype: p=0.0074; Genotype x Peak Amplitude interaction: $F_{3, 63}$=2.979; p=0.0381; WT n=11; KO n=10; Tone: WT *vs.* KO: p=0.0098; Trace: WT *vs.* KO: p=0.0441). **K.** Tone test: comparison between freezing and dCA1 responses relative to tone onset (Genotype x Fluorescence (5-10sec): $F_{149, 3129}$ = 2.093; P<0.0001). **L.** Tone test: comparison between freezing and dCA1 responses relative to the end of the tone (i.e., trace onset Genotype x Fluorescence (10-40sec) $F_{899, 17980}$ = 1.101; P=0.0209).

Data shown at mean ± SEM. *: p<0.05; **: p<0.01; ***: p<0.001; * represents genotype effect. # represents genotype x variable interaction.

Figure 3. *Cntnap2* KO mice dicsplay impaired relational/declarative memory.

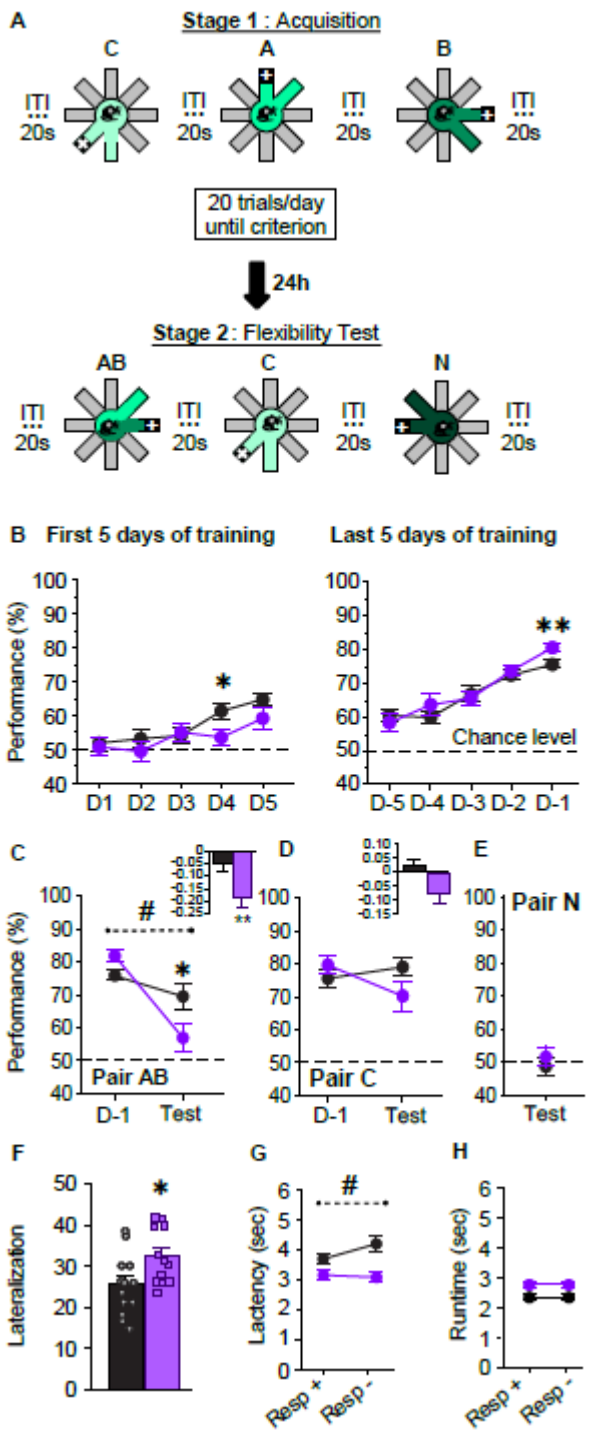

A. Experimental design: Relational/Declarative memory task. ITI: Inter-trial interval; +: represent reward location within each pair of arms. **B.** Average correct answers for WT (black; n = 12) and *Cntnap2* KO mice (purple; n = 13) for pairs A, B, and C during the 5 first days of acquisition (left panel; day (D); D4: Genotype: p=0.0123), and the last 5 days of acquisition (right panel; D-5: 5 days before they reach learning criterion; D-1: Genotype: p=0.0082). **C.** Comparison of the correct answers during the last day of training (D-1) averaged on pairs A and B, and during the flexibility test on the recombined pair AB (Genotype X Performance interaction: $F_{1,29}$=10.953, p=0.0025). Inset: D-1 *vs.* Test performance index on pairs AB (Genotype: p=0.0035). **D.** Comparison of the correct answers on pair C during the last day of training (D-1) and the flexibility test. Inset: D-1 *vs.* Test performance index for Pair C. **E.** Average performance on the new pair N during the flexibility test. **F.** Maximum lateralization index during stage 1 (average performance pairs A and B (left baited) vs Pair C (right baited); Genotype: p=0.0213). **G.** Average decision latencies for correct (+) and incorrect (-) answers throughout training (Genotype X Response interaction: $F_{1,31}$=7.960, p=0.0083). **H.** Average runtimes for correct (+) and incorrect (-) answers throughout training.

Dashed line illustrates chance level. Data shown at mean ± SEM. *: p<0.05; **: p<0.01; # shows genotype x performance interaction.

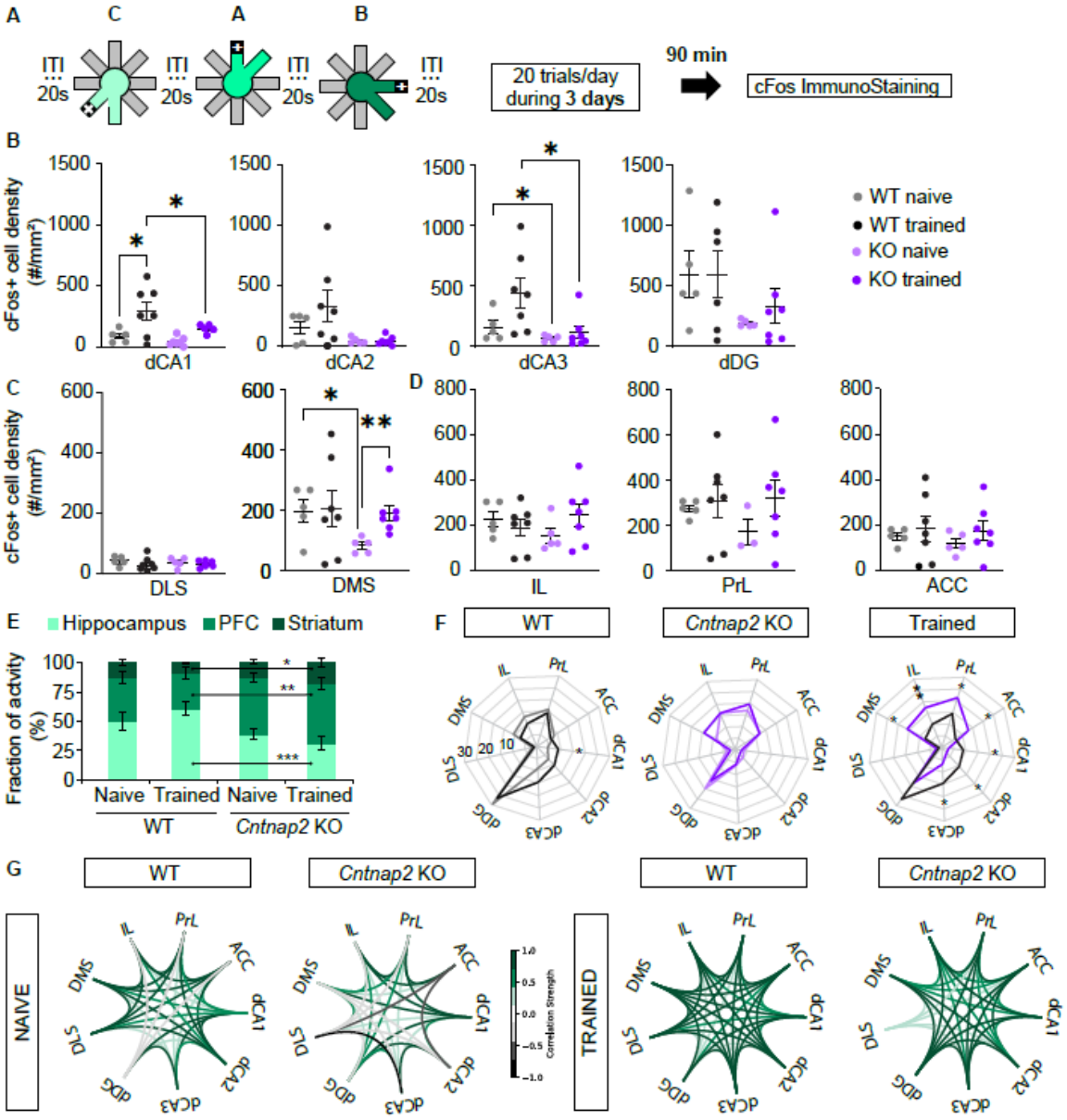

Figure 4. imbalance in learning-induced functional connectivity in *Cntnap2* KO mice

A. Experimental design: cFos levels were quantified 90min after the 3rd training session of the Relational/Declarative memory task. ITI: Inter-trial interval; + represent reward location within each pair of arms. **B.** number of cFos-positive neurons (cell density/mm^2) in the hippocampus subfields: dCA1 (WT naïve vs Trained: p=0.0491; Trained WT vs. KO: p=0.0129), dCA2, dCA3 (Naive WT vs. KO: p=0.0400; Trained WT vs. KO: p=0.0454), dDG for naïve (light colors) and trained (dark colors) WT (grey/black) and *Cntnap2* KO (purple) groups. **C.** number of cFos-positive neurons (cell density/mm^2) in the striatum: DMS (Naive WT vs. KO: p=0.0189; KO Naïve vs Trained: p=0.0085), DLS. **D.** number of cFos-positive neurons (cell density/mm^2) in the prefrontal cortex: IL, PrL, ACC. **E.** Proportion of activity for each structure compared to the total activity measured (percentage; Trained WT vs. KO: Hippocampus: p=0.00023; PFC:

p=0.00139; Striatum: p=0.02895). **F.** Proportion of the activity each subfield within the total network activity (percentage), in WT mice (naïve vs trained, left panel; dCA1: p=0.0382), in *Cntnap2*KO mice (Naïve vs trained, middle panel), and in trained mice (WT vs *Cntnap2* KO mice, dCA1: p=0.0183; dCA2: p=0.0201; dCA3: p=0.0307; ACC: p=0.0378; DMS: p=0.0303; IL: p=0.0060; PrL: p=0.0476; right panel, same data as in left and middle panels). **G.** Pairwise between-structure correlation strength of cFos cell density.

Data shown at mean ± SEM. *: p<0.05; **: p<0.01; # shows genotype x performance interaction.

1. DSM-5, Association American Psychiatric (2013) Diagnostic and statistical manual of mental disorders : DSM-5.

2. Bal VH, Kim SH, Cheong D, Lord C (2015) Daily living skills in individuals with autism spectrum disorder from 2 to 21 years of age. Autism 19:774–784. https://doi.org/10.1177/1362361315575840

3. Banker SM, Gu X, Schiller D, Foss-Feig JH (2021) Hippocampal contributions to social and cognitive deficits in autism spectrum disorder. https://doi.org/10.1016/j.tins.2021.08.005

4. Eichenbaum H (2014) Time cells in the hippocampus: a new dimension for mapping memories. Nat Rev Neurosci 15:732–44. https://doi.org/10.1038/nrn3827

5. Bartsch T, Döhring J, Rohr A, et al (2011) CA1 neurons in the human hippocampus are critical for autobiographical memory, mental time travel, and autonoetic consciousness. Proc Natl Acad Sci U S A 108:17562–17567. https://doi.org/10.1073/pnas.1110266108

6. Barrientos SA, Tiznado V (2016) Hippocampal CA1 subregion as a context decoder. Journal of Neuroscience 36:6602–6604. https://doi.org/10.1523/JNEUROSCI.1107-16.2016

7. Eichenbaum H (2004) Hippocampus : Cognitive Processes and Neural Representations that Underlie Declarative Memory The hippocampus serves a critical role in declarative. Neuron 44:109–120

8. Sellami A, Al Abed AS, Brayda-Bruno L, et al (2017) Temporal binding function of dorsal CA1 is critical for declarative memory formation. Proc Natl Acad Sci U S A 114:. https://doi.org/10.1073/pnas.1619657114

9. Minor GN, Hannula DE, Gordon A, et al (2023) Relational memory weakness in autism despite the use of a controlled encoding task. Front Psychol 14:. https://doi.org/10.3389/fpsyg.2023.1210259

10. Bowler D, Gaigg S, Lind S (2011) Memory in autism: Binding, self and brain. In: Researching the Autism Spectrum: Contemporary Perspectives. Cambridge University Press, pp 316–346

11. Vogel DHV, Jording M, Esser C, et al (2022) Temporal binding of social events less pronounced in individuals with Autism Spectrum Disorder. Sci Rep 12:. https://doi.org/10.1038/s41598-022-19309-y

12. Maister L, Plaisted-Grant KC (2011) Time perception and its relationship to memory Autism Spectrum Conditions. Dev Sci 14:1311–1322. https://doi.org/10.1111/j.1467-7687.2011.01077.x

13. Buonomano D V., Buzsáki G, Davachi L, Nobre AC (2023) Time for Memories. In: Journal of Neuroscience. Society for Neuroscience, pp 7565–7574

14. Peñagarikano O, Geschwind DH (2012) What does CNTNAP2 reveal about autism spectrum disorder? Trends Mol Med 18:156–163. https://doi.org/10.1016/j.molmed.2012.01.003

15. Peñagarikano O, Abrahams BS, Herman EI, et al (2011) Absence of CNTNAP2 leads to epilepsy, neuronal migration abnormalities, and core autism-related deficits. Cell 147:235–46. https://doi.org/10.1016/j.cell.2011.08.040

16. Blanchard RJ, Flannelly KJ, Blanchard DC (1986) Defensive behavior of laboratory and wild Rattus norvegicus. J Comp Psychol 100:101–107. https://doi.org/10.1037/0735-7036.100.2.101

17. Al Abed AS, Sellami A, Potier M, et al (2020) Age-related impairment of declarative memory: linking memorization of temporal associations to GluN2B redistribution in dorsal CA1. Aging Cell 1–12. https://doi.org/10.1111/acel.13243

18. Simon DM, Wallace MT (2016) Dysfunction of sensory oscillations in Autism Spectrum Disorder. Neurosci Biobehav Rev 68:848–861

19. Sellami A, Abed A, Brayda-Bruno L, et al (2018) Protocols to Study Declarative Memory Formation in Mice and Humans: Optogenetics and Translational Behavioral Approaches. Bio Protoc 8:. https://doi.org/10.21769/BioProtoc.2888

20. Mingaud F, Le Moine C, Etchamendy N, et al (2007) The hippocampus plays a critical role at encoding discontiguous events for subsequent declarative memory expression in mice. Hippocampus 17:264–70. https://doi.org/10.1002/hipo.20262

21. Uddin LQ, Supekar K, Lynch CJ, et al (2015) Brain state differentiation and behavioral inflexibility in autism. Cerebral Cortex 25:4740–4747. https://doi.org/10.1093/cercor/bhu161

22. White NM, McDonald RJ (2002) Multiple parallel memory systems in the brain of the rat. Neurobiol Learn Mem 77:125–84. https://doi.org/10.1006/nlme.2001.4008

23. Buzsáki G, Tingley D (2018) Space and Time: The Hippocampus as a Sequence Generator. Trends Cogn Sci 22:853–869

24. Tsien JZ, Huerta PT, Tonegawa S (1996) The Essential Role of Hippocampal CA1 NMDA Receptor – Dependent Synaptic Plasticity in Spatial Memory. 87:1327–1338

25. Chowdhury N, Quinn JJ, Fanselow MS (2005) Dorsal hippocampus involvement in trace fear conditioning with long, but not short, trace intervals in mice. Behavioral Neuroscience 119:1396–1402. https://doi.org/10.1037/0735-7044.119.5.1396

26. Chang Q, Gold PE (2003) Switching memory systems during learning: changes in patterns of brain acetylcholine release in the hippocampus and striatum in rats. J Neurosci 23:3001–5

27. Etchamendy N, Desmedt A, Cortes-Torrea C, et al (2003) Hippocampal lesions and discrimination performance of mice in the radial maze: sparing or impairment depending on the representational demands of the task. Hippocampus 13:197–211. https://doi.org/10.1002/hipo.10055

28. Ferbinteanu J (2016) Contributions of hippocampus and striatum to memory-guided behavior depend on past experience. Journal of Neuroscience 36:6459–6470. https://doi.org/10.1523/JNEUROSCI.0840-16.2016

29. Zhang L, Chen P, Schafer M, et al (2022) A specific brain network for a social map in the human brain. Sci Rep 12:. https://doi.org/10.1038/s41598-022-05601-4

30. Brewin CR (2011) The Nature and Significance of Memory Disturbance in Posttraumatic Stress Disorder. https://doi.org/101146/annurev-clinpsy-032210-104544 7:203–227. https://doi.org/10.1146/ANNUREV-CLINPSY-032210-104544

31. Al Abed AS, Ducourneau E-G, Bouarab C, et al (2020) Preventing and treating PTSD-like memory by trauma contextualization. Nat Commun 1–9. https://doi.org/10.1038/s41467-020-18002-w

32. Al Abed AS, Allen TV, Ahmed NY, et al (2024) Parvalbumin interneuron activity in autism underlies susceptibility to PTSD-like memory formation. iScience 27:109747. https://doi.org/10.1016/j.isci.2024.109747

33. Rumball F, Happé F, Grey N (2020) Experience of Trauma and PTSD Symptoms in Autistic Adults: Risk of PTSD Development Following DSM-5 and Non-DSM-5 Traumatic Life Events. Autism Research 13:2122–2132. https://doi.org/10.1002/AUR.2306

34. Mocle AJ, Ramsaran AI, Jacob AD, et al (2024) Excitability mediates allocation of pre-configured ensembles to a hippocampal engram supporting contextual conditioned threat in mice. Neuron 112:1487-1497.e6. https://doi.org/10.1016/J.NEURON.2024.02.007

35. Rashid AJ, Yan C, Mercaldo V, et al (2016) Competition between engrams influences fear memory formation and recall. Science (1979) 353:383–387. https://doi.org/10.1126/science.aaf0594

36. Leal SL, Yassa MA (2015) Neurocognitive Aging and the Hippocampus across Species. Trends Neurosci 38:800–12. https://doi.org/10.1016/j.tins.2015.10.003

37. Etchamendy N, Konishi K, Pike GB, et al (2012) Evidence for a virtual human analog of a rodent relational memory task: a study of aging and fMRI in young adults. Hippocampus 22:869–80. https://doi.org/10.1002/hipo.20948

38. Wang J, Christensen D, Coombes SA, Wang Z (2024) Cognitive and brain morphological deviations in middle-to-old aged autistic adults: A systematic review and meta-analysis. Neurosci Biobehav Rev 163

39. Marighetto, Brayda-bruno, Etchamendy (2011) Studying the Impact of Aging on Memory Systems : Contribution of Two Behavioral Models in the Mouse. https://doi.org/10.1007/7854

40. Hollunder B, Ostrem JL, Sahin IA, et al (2024) Mapping dysfunctional circuits in the frontal cortex using deep brain stimulation. Nat Neurosci 27:573–586. https://doi.org/10.1038/s41593-024-01570-1